Escola de Primavera de Transição e Turbulência
Blumenau 2022

ABCM
Associação Brasileira de Engenharia e Ciências Mecânicas

13th Spring School on Transition and Turbulence
September 19th-23rd, 2022, Blumenau, SC, Brazil

EPTT-2022-0073
LES SIMULATION OF A WAVE-PLATE DEMISTER

Vinícius Basso de Godoy*
viniciusbassodegodoy@gmail.com

Bárbara Braatz Vetter*
barbarabraatz.vetter@gmail.com

Joseph Meyer*
josephm@furb.br

Jonathan Utzig*
jutzig@furb.br

Henry França Meier*
meier@furb.br
*Chemical Engineering Department – University of Blumenau (FURB) – Blumenau – SC

Abstract. *The mist elimination process is commonly used in many industrial sectors such as chemical, oil and gas, desalination, and mining industry. The equipment known as demister or mist eliminator is designed to remove liquid droplets from a gas stream by performing an intervention on the force balance of the drops. For the design and study of demisters, Computational Fluid Dynamics (CFD) is a valuable tool to predict the equipment behavior with relatively low cost. Effort has been made to numerically solve for separation efficiency using predominantly Reynolds Averaged Numerical Simulation (RANS) approach, whereas few studies considered LES on their analysis. Thus, the objective of this work is to analyze the performance of a wave-plate demister using LES approach rather than RANS by determining the separation efficiency of the equipment at different gas velocities and liquid volume fraction. To achieve this objective, numerical simulations will be performed by using the Eulerian-Lagrangian method for the two-phase flow considering the WALE turbulence model for the LES sub-grid scales. The demister performance is evaluated by means of separation efficiency. Results show that the demister used in this study works at best with higher concentration of droplets around 10% of volume fraction and at medium air velocities around 3.5 m/s, reaching a number separation efficiency of 99.11%. Additionally, the mesh quality analysis proved to be an easy method to conduct in a LES simulation.*

Keywords: *Computational Fluid Dynamics, mist elimination, Large Eddy Simulation, turbulent kinetic energy*

1. INTRODUCTION

Mist elimination process, which consists in eliminating liquid droplets from a gas stream, is commonly used in many industrial sectors such as energy, chemical, oil and gas, desalination, and mining industry (LI et al., 2020; VENKATESAN, KULASEKHARAN, INIYAN, 2014; YANG et al., 2021). The equipment designed to remove these liquid droplets from a gas stream is known as demister or mist eliminator. According to Yang et al. (2021), the most common mist eliminators can be divided into 3 categories: wave-plate, cyclone, and wire mesh. It can be said that all mist eliminators are based on the same separation principle of performing an intervention on the gravitational and drag forces of the drop (STEWART and ARNOLD, 2008). In the case of cyclone-type demisters, the centrifugal force is added to the force balance by imposing a tangential flow on the inlet. On the other hand, both wire mesh and wave-plate demisters utilize some form of physical barrier, commonly referred to as a target, to provoke several impingements of droplets on its surface. This mechanism promotes the formation of a conglomerate of droplets on the target and it ends up boosting the size of the original droplets. As these enlarged drops hold greater gravitational force, they acquire sufficient momentum to inertially separate from the gas streamlines, promoting the desired liquid separation.

The wave-plate demister has some advantages over other types such as simple construction with low pressure drop, fine droplet separation (up to 1 μm) and they are less prone to clogging. They consist in several plates bended together forming channels for the gas to flow. While these channels force the gas to flow in a zigzag manner, the liquid droplets acquire sufficient momentum to inertially separate from the gas stream, causing wall impingement, coalescence, and liquid drain (VENKATESAN, KULASEKHARAN, INIYAN, 2014). Since this equipment forces the gas to flow larger distances in higher velocities, one of the challenges regarding its design is to achieve a good separation while maintaining

low pressure drop. According to Kavousi, Behjat and Shahhosseini (2013), the separation efficiency of this demister type is affected by different factors, such as fluid inlet velocity, vane geometry and droplet mass fraction. One simple modification on the geometry of the wave-plate demister such as the addition of drainage channels or hooks can enhance the separation efficiency while avoiding liquid flooding on walls and re-entrainment of collected liquid drops (JAMES et al., 2003).

For the design of demisters, Computational Fluid Dynamics (CFD) is a valuable tool to predict the equipment behavior with relatively low cost. In this regard, many computational studies have been executed during the past thirty years. Wang and James (1998) performed a numerical study in order to calculate separation efficiency of two wave-plate demisters using the Eulerian-Lagrangian approach in which is considered when there is a low concentration of droplets. The authors concluded that the results from the low Re k-ϵ model coincided better with the experimental data when comparing with the results from standard k-ϵ model. However, large discrepancies still exist between numerical prediction of efficiency and experimental data. The authors argue that these differences are probably due to lack of turbulent dispersion effects of the simulations.

James et al. (2003) studied the effect of drainage channels or hooks on demister performance using standard k-ϵ turbulence model. The motion of liquid droplets was modelled using the Eulerian-Lagrangian method. The authors found that the separation efficiency of demisters with and without drainage hooks increase with the bulk gas velocity. Additionally, the presence of drainage hooks increases equipment performance substantially compared to mist eliminators with no hooks and similar operating conditions. The authors also suggest that a more efficient way of increasing separation efficiency is to add these drainage channels instead of increasing bulk gas velocity.

Zhao, Jin and Zhong (2007) investigated the influences of many geometrical parameters and operating conditions on separation efficiency using a statistical method called response surface methodology with CFD simulations. The authors considered the Eulerian-Lagrangian approach to calculate the motion of the fluids with the presence of the drag force but no turbulent dispersion effect. They developed a prediction model of separation efficiency that can be used to determine the most influential parameters on demister performance. For example, the authors found that while increasing the gas velocity at the inlet promotes better separation, a reduction on separation efficiency is observed when the distance between plates is increased.

Guan et al. (2016) studied the penetration of droplets of different sizes in a zigzag demister while considering the effect of coalescence on separation efficiency. For the two-phase flow, the author considered the Eulerian-Lagrangian approach with standard k-ϵ turbulence model. The numerical simulations agreed well with experimental data except at high gas velocity. The results show significant increase on separation efficiency when adding the effect of coalescence on the simulations, particularly at lower velocities. Additionally, the authors concluded that while droplets above 22.5 μm are mainly collected by the plate walls, droplets between 7.5 and 22.5 μm tends to be collected more by the effect of coalescence.

Li et al. (2020) evaluated numerically the separation efficiency of four chevron demisters in order to determine the ideal one. The differences between them are due to different drainage hook configuration and all types have four stages or flow turns. The two-phase flow was modelled using Eulerian-Lagrangian approach with the addition of Eulerian Wall Film (EWF) model, Eddy Interaction Model (EIM) and Discrete Random Walk (DRW). The last two models insert interactions of eddies from the continuous phase with the discrete phase, providing better computational result for smaller droplets. For turbulence closure, realizable k-ϵ model was considered. The results revealed that large drops are mainly captured at the first two stages and small droplets are likely to pass through the equipment as they have less momentum. The best demister type proved to be the type D (with single hook per turn) at the cost of higher-pressure loss.

As can be observed by the aforementioned studies, much effort has been made to numerically solve for separation efficiency using predominantly Reynolds Averaged Numerical Simulation (RANS) method, whereas few studies considered Large Eddy Simulation (LES) on their analysis. Thus, the objective of this work is to analyze the performance of a wave-plate demister using LES approach rather than RANS by determining the separation efficiency of the equipment at different gas velocities and liquid volume fraction. This study may also be used as a practical guide to set up a basic LES case. To achieve these objectives, numerical simulations will be performed by using the Eulerian-Lagrangian method for the two-phase flow considering the WALE turbulence model for the LES sub-grid scales. The demister performance is evaluated by means of separation efficiency. Additionally, in order to determine if the mesh refine is sufficient for a proper LES simulation, a quantitative analysis that verifies the amount of turbulent kinetic energy being resolved by the mesh is discussed.

2. NUMERICAL METHODOLOGY

A wave-plate demister with drainage hooks is considered for the numerical analysis and its profile is shown in Figure 1. The demister contains 10 channels in total with a perpendicular distance between plates l_p of 9.73 mm and distance between hook wall and plate wall l_h of 4.57 mm. Total height H of the equipment is equal to 178 mm and each channel contains a depth W of 93.5 mm. The area painted in gray was considered for generating the CFD geometry, as this simplified model assures good orthogonal quality mesh.

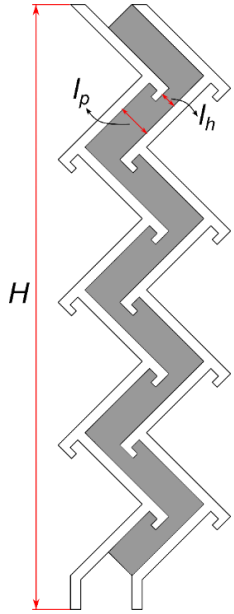

Figure 1. Channel profile geometry of the wave-plate demister with drainage hooks.

Calculations were performed using the commercial solver ANSYS Fluent 19.1. As can be seen by the many studies from the literature, the Eulerian-Lagrangian approach was selected as a common solving approach for the demister case. This means that the gas phase flow field is solved as an eulerian phase, and the motion of liquid droplets is solved numerically as a lagrangian phase. For the calculation of the continuous phase, the LES method with Wall-Adapting Local Eddy-Viscosity (WALE) sub-grid scale (SGS) turbulence model is considered. Three inlet velocities (low, medium, high as 1.0, 3.5 and 10 m/s, respectively) were selected with two liquid volume fractions at the inlet (1 and 10%). Then, the separation efficiency of each case is addressed and discussed. Some reasonable assumptions were made in order to simplify the problem:

- As the depth of the wave-plate wall is much larger than the other two dimensions, the flow would be considered as two dimensional. However, since the present study is performing a LES simulation case and large-scale turbulent eddies are three dimensional in nature, a three-dimensional demister model is considered. This model consists of a small slice of a single demister channel with the boundaries perpendicular to the depth direction treated as symmetry planes. The model with detailed geometry information is depicted in Figure 2;
- The interaction among droplets is negligible;
- Re-entrainment of droplets was not considered;
- When droplets collide on the walls, they are assumed to be automatically collected and no rebound into the gas flow occurs;
- Droplets are treated as perfect spheres;
- No heat and mass transfer occur between phases.

Liquid with modified physical properties is considered for the discrete phase and air is considered for the continuous phase. The density of the liquid is considered the same as the density of water (998.2 kg/m³) and the density of the air is calculated by ideal gas law with the viscosity of 1.05 x 10^{-5} Pa·s. Viscosity and surface tension of the liquid are equal to 1.074 x 10^{-3} Pa·s and 27.926 mN/m, respectively.

To select the ideal mesh size, some steady-state RANS calculations were performed using $k-\omega$ SST turbulence model. We considered the case in which inlet air velocity is equal 10 m/s for this analysis because it demands a high-quality mesh to calculate the turbulence in domain (LI et al. 2020). The pressure drop of these test cases are shown in Figure 3. It can be seen that the pressure drop with a mesh above 232,056 cells has almost the same value for pressure drop with 523,632 cells mesh, indicating that the mesh with 232,056 cells is ideal for this study. The first layer of cells at the walls of the domain is set to be equal to 20 μm with a growth factor of 1.2. Therefore, the resulting Y plus remains below the critical value of 5 for correct calculation of the boundary layer.

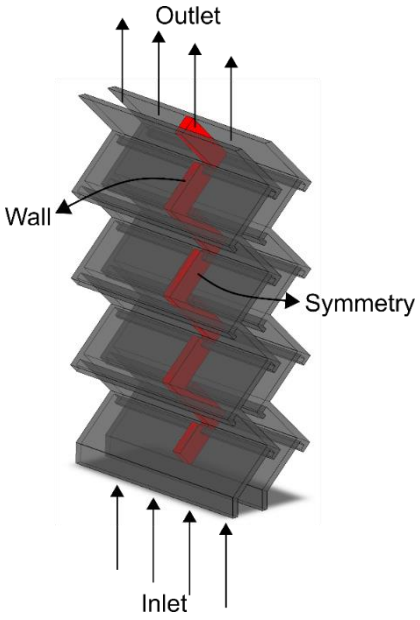

Figure 2. Three-dimensional demister model colored in red used on the simulations.

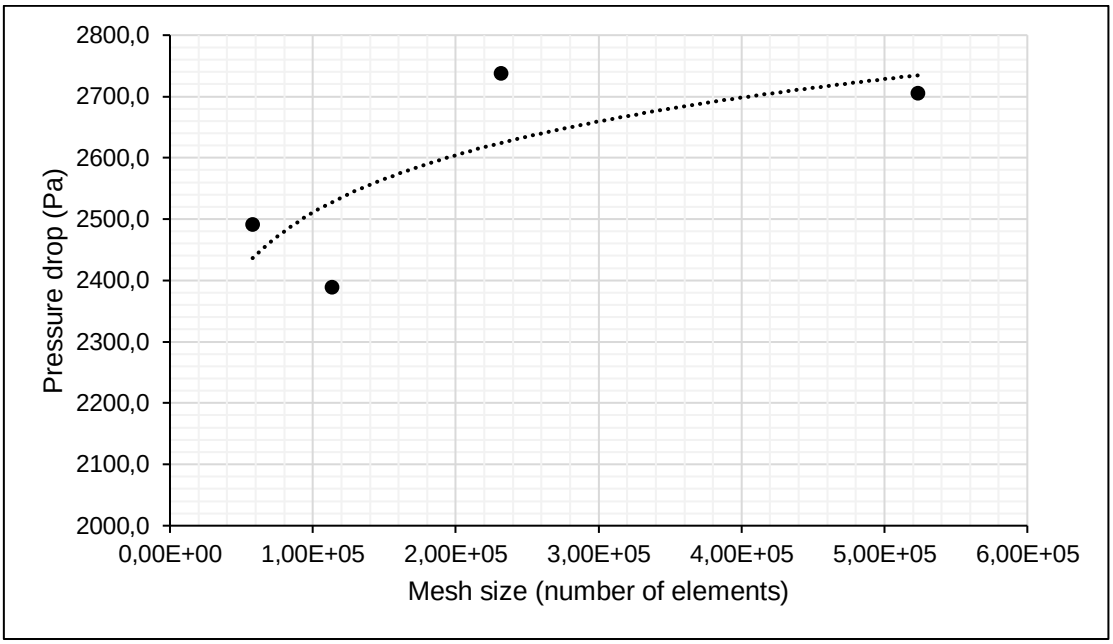

Figure 3. Pressure drop variation with mesh size using steady state RANS simulation.

The transport equations in LES simulation are derived for the large eddies by spatially filtering the Navier-Stokes equation, which variations of the fluctuating variable occurring on small scales are removed by the filter and the large-scale variation is preserved. The filtered equations expressing conservation of mass and momentum in a Newtonian incompressible flow can be written as

$$\frac{\partial \overline{u_i}}{\partial x_i} = 0 \tag{1}$$

$$\frac{\partial(\rho\overline{u_i})}{\partial t} + \frac{\partial\rho\left(\overline{u_i u_j}\right)}{\partial x_j} = \frac{\partial \bar{p}}{\partial x_i} + 2\frac{\partial\left(\mu\overline{S_{ij}}\right)}{\partial x_j} - \frac{\partial \tau_{ij}}{\partial x_j} \tag{2}$$

$$\overline{S_{ij}} = \frac{1}{2}\left(\frac{\partial \overline{u_j}}{\partial x_i} + \frac{\partial \overline{u_i}}{\partial x_j}\right) \tag{3}$$

$$\tau_{ij} = \rho\left(\overline{u_i u_j} + \bar{u}_i \bar{u}_j\right), \tag{4}$$

where ρ is the density of the fluid, $\bar{u}_i$ is the filtered velocity, $\bar{p}$ is the filtered pressure, μ is the viscosity of the fluid, $\overline{S_{ij}}$ is the resolved scale strain rate tensor and τ_{ij} is the unknown SGS stress tensor that needs to be modelled. The sub-grid scale turbulence models in ANSYS Fluent employ the Boussinesq hypothesis as in the RANS models, written as

$$\tau_{ij} - \frac{1}{3}\tau_{kk}\delta_{ij} = -2\mu_t \bar{S}_{ij}, \tag{5}$$

where μ_t is the SGS turbulent viscosity or eddy viscosity. In this study, the eddy viscosity is determined by the WALE model

$$\mu_t = \rho L_{SGS}^2 \frac{\left(S_{ij}^d S_{ij}^d\right)^{3/2}}{\left(\bar{S}_{ij}\bar{S}_{ij}\right)^{5/2} + \left(S_{ij}^d S_{ij}^d\right)^{5/4}}, \tag{6}$$

which is designed for wall bounded flows. In the previous equation, L_{SGS} is the sub-grid length scale, defined as the size of an eddy that has the same TKE as the average of all eddies smaller than the cell size. L_{SGS} and S_{ij}^d are defined, respectively, as

$$L_{SGS} = min\left(\kappa d, C_w V^{1/3}\right), \tag{7}$$

$$S_{ij}^d = \frac{1}{2}\left(\bar{g}_{ij}^2 + \bar{g}_{ji}^2\right) - \frac{1}{3}\delta_{ij}\bar{g}_{kk}^2, \qquad \bar{g}_{ij} = \frac{\partial \bar{u}_i}{\partial x_j}, \tag{8}$$

where κ is the von Kármán constant, d is the distance to the closest wall, C_w is the WALE constant and it is equal to 0.325, and V is the volume of the computational cell.

The trajectory of the droplets is obtained by integrating the force balance equation which includes drag, buoyancy, and gravitational forces. The movement of droplets using a Lagrangian reference frame can be written as

$$\frac{d\vec{u}_p}{dt} = F_D\left(\vec{u} - \vec{u}_p\right) + \frac{\vec{g}\left(\rho_p - \rho\right)}{\rho_p} + \vec{F}, \tag{9}$$

where $\vec{u}$ is the velocity of the continuous phase, $\vec{u}_p$ is the velocity of droplets, ρ_p is the density of droplets; ρ is the density of continuous fluid, $\vec{F}$ is the additional forces of the gas acting on the droplets, and $F_D\left(\vec{u} - \vec{u}_p\right)$ is the drag force of gas on the liquid droplet. In Eq. 9, F_D is defined as

$$F_D = \frac{18\mu}{\rho_p D_p^2} \cdot \frac{C_D Re}{24}, \tag{10}$$

where D_p is the diameter of the drop, Re is the relative Reynolds number defined as

$$Re = \frac{\rho D_p \left|\vec{u}_p - \vec{u}\right|}{\mu}, \tag{11}$$

and C_D is the damping coefficient.

To assess the quality of the mesh for a LES simulation, one simple method is to calculate the turbulent kinetic energy (TKE), defined as

$$k_{res} = \frac{1}{2}\left(\overline{u'u'} + \overline{v'v'} + \overline{w'w'}\right), \tag{12}$$

where k_{res} is the TKE that is resolved by the mesh, and u', v' and w' are the fluctuating velocities at the X, Y and Z directions, respectively. On the other hand, the SGS TKE (k_{SGS}) represents the TKE of the eddies smaller than the cell size, modelled by the SGS WALE model and calculated as

$$k_{SGS} = \left(\frac{\mu_t}{\rho L_{SGS}}\right)^2. \tag{13}$$

At last, we can verify if the mesh refine is sufficient for the LES simulation by calculating the fraction of the TKE that is resolved by the mesh, defined as

$$f = \frac{k_{res}}{k_{res} + k_{SGS}}. \tag{14}$$

A mesh that achieves a value of 0.8 in the entire domain may be considered sufficient for a LES simulation, although some areas (near-wall area, for example) may fail to meet this arbitrary criterion due to high resolution demand (POPE, 2000).

Since, for a LES case, it is necessary to provide accurate information about the flow field, the RANS initial guess strategy was implemented. This strategy utilizes the steady-state flow field calculated by a RANS simulation to generate the instantaneous velocity field needed for the LES simulation. This ends up producing a more realistic initial flow field and helps reducing LES simulation time. In this strategy, $k-\omega$ SST turbulence model is chosen for resolving the Reynolds stresses derived by averaging the Navier-Stokes equations. Thus, the ratio or fraction of TKE resolved by the mesh is determined in this study by the following steps:

1. A $k-\omega$ SST steady state RANS simulation without discrete phase is performed starting with first order discretization schemes and ending with second order discretization schemes plus PRESTO! for pressure interpolation scheme. Convergence with low residuals criterion is desired, although it is not mandatory;
2. As previously noted, the simulation results from the RANS simulation are used for initializing the LES simulation by generating an instantaneous velocity field. The command used for achieving this step in ANSYS Fluent is “solve/initialize/init-instantaneous-vel” after performing the RANS calculation;
3. Then, a LES simulation without discrete phase using SGS WALE model is run, and a velocity probe is inserted near the outlet of the domain. This velocity probe is monitored and sampled at every time step. A statistical steady state, defined as a state in which the variable of interest does not change in time and remains around its mean value, is needed;
4. When a statistical steady state is reached, the “Data Sampling for Time Statistics” in ANSYS Fluent is applied with a time step interval of 5 until the contour plot of the ratio of resolved TKE (step number 5) does not change drastically in time. This tool enables the calculation of RMSE velocities used in Eq. 12;
5. Calculation of the new field variable f on a post-processing software (CFD Post in our case) on a contour plot to verify regions of low values of resolved TKE ratio. As previously commented, for a LES case, a good mesh has a recommended value of 0.8 in all regions. If not, a local refinement may be necessary.

After concluding these steps, the liquid phase is added to the problem. For the liquid phase, the Eulerian-Lagrangian Discrete Phase Model (DPM) was selected and two volume fractions at the inlet (1 and 10%) were chosen. Since a LES simulation requires a transient state, an unsteady particle tracking is applied on the liquid droplets. In order to reduce computational time and to simplify the problem, droplets are injected only for a few time steps and the simulation continues until no particles are present in the domain. Additionally, the Discrete Random Walk (DRW) method was also applied and “trap” boundary condition on the wall was selected for the discrete phase. To compare performance between cases, the separation efficiency φ, written as

$$\varphi = \frac{M_{inlet} - M_{outlet}}{M_{inlet}} \times 100, \tag{15}$$

was calculated. In Eq. 15, M_{inlet} is defined as the mass of droplets that passes through the outlet plane and M_{inlet} is the mass of droplets that is injected at the inlet.

The size of the droplets follows the Rosin-Rammler (R-R) distribution with droplets being injected into the gas flow by the inlet surface. The surface type was selected for the method of injection, resulting in a uniform distribution of particles over the inlet surface. The mass fraction of droplets with a diameter greater than D is given by

$$W_D = e^{-(D/\bar{D})^n}, \tag{16}$$

where $\bar{D}$ is the size constant, and n is the size distribution parameter. In this study, the size constant equals 20 µm. The selected minimum diameter, maximum diameter and size distribution parameter were 1 µm, 100 µm, and 1.2, respectively. This value selection generates a broad distribution over the entire range, with most droplets located at the low size diameter range (around 20µm) as
Figure 4 illustrates below.

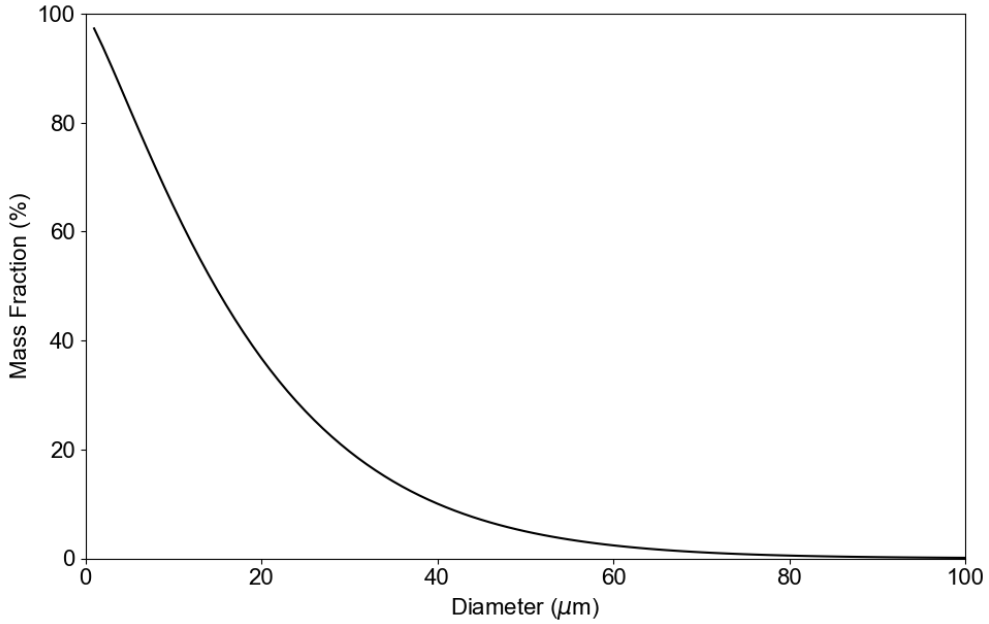

Figure 4. Rosin-Rammler distribution of the droplets at the inlet.

3. RESULTS AND DISCUSSION

Firstly, the quantitative analysis of resolved TKE ratio is discussed only for each velocity case (1.0, 3.5 and 10 m/s), since this part does not yet apply DPM calculations for the liquid drops. Figure 5 shows the contour plots of resolved TKE ratio from all velocity cases. These results show that most of the domain reaches the value of 0.8, indicating that the mesh is sufficient for a good LES simulation. However, some regions near the inlet exhibited low values of resolved TKE ratio exclusively for the low and medium velocities (1.0 and 3.5 m/s, respectively). This indicates that high velocity flow produces higher turbulence energy spectrum with larger eddies when compared to a low velocity flow. Therefore, these larger eddies are easily resolved by the mesh (i.e., enough spatial resolution is provided). For the low and medium velocity cases, when the flow reaches the first drainage hook and it is forced to change direction, shear layer flow occurs and many eddies are generated, increasing the ratio of resolved TKE by the mesh beyond that point and reaching values above 0.8.

Since most of the domain reaches values of f above 0.95 for all cases, the present mesh with 232,056 cells is considered sufficient for the LES simulation of this study. However, to achieve an even higher mesh quality, it is recommended to address a new local refinement at the entry region around the first hook for the low and medium velocity cases. For the sake of simplicity, this will not be conducted in this study. Therefore, the current mesh is still considered the ideal one.

After performing the mesh quality analysis, we applied the discrete phase into the stabilized results of the LES simulations conducted above. As mentioned previously, it was considered two different liquid volume fractions at the inlet (1 and 10%) for each velocity, resulting in a total of 6 cases. Table 1 shows the separation efficiency for each case. It can be noted that the separation efficiency based on mass of droplets is not a proper variable for comparison between cases in this study since its values are very close to each other. Nevertheless, some interesting findings still can be stated. The cases III and IV, in which air velocity is equal to 3.5 m/s, presented the highest values, indicating that this inlet condition is the optimal one for separating liquid droplets from an air stream. When comparing the same air velocity with different liquid volume fractions, we can notice that this equipment works at best with higher concentration of droplets. A possible explanation for the aforementioned statement is that increasing volume fraction at the inlet increases the amount of mass at each parcel of particles, resulting in a higher number of heavier/bigger droplets (since the total number of droplets is constant). These heavier/bigger droplets tend to be captured more easily by the demister, since they possess

more gravitational force. Another variable that can evaluate the separation process is the separation efficiency based on number of droplets, written as

$$\varphi_{number} = \frac{N_{drops}^{inlet} - N_{drops}^{outlet}}{N_{drops}^{inlet}} \times 100, \tag{17}$$

where N_{drops}^{outlet} is the number of droplets that passes through the outlet plane and N_{drops}^{inlet} is the number of droplets that is injected at the inlet. Table 2 presents the number separation efficiency for each case.

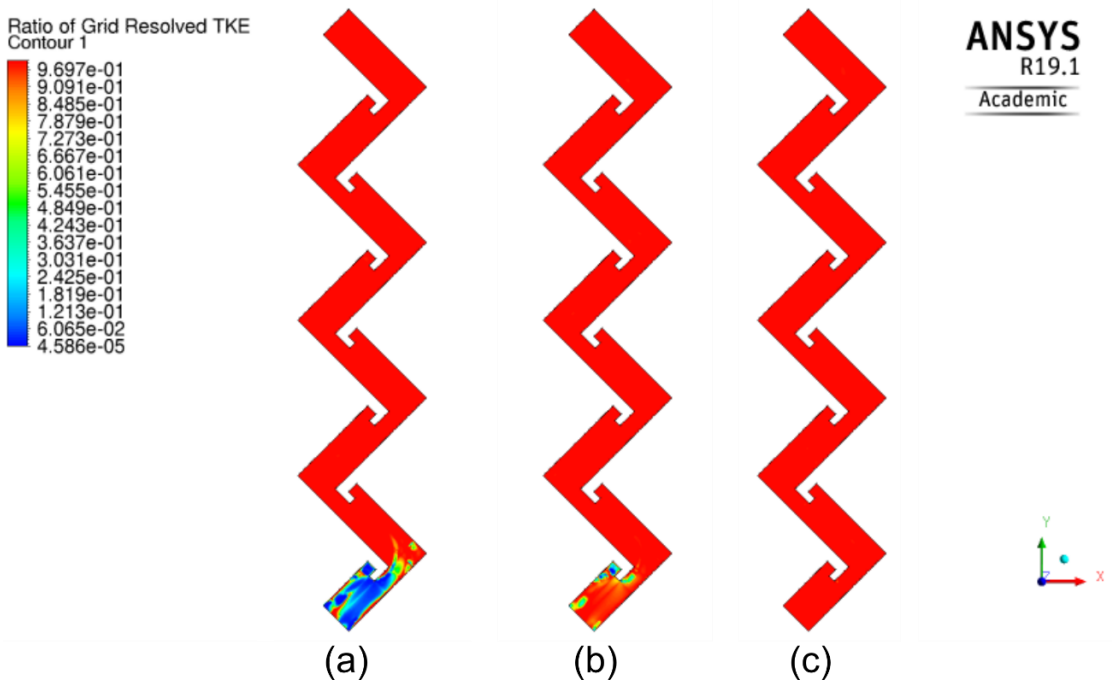

Figure 5. Ratio of resolved TKE from each velocity case. (a) represents the low velocity (1.0 m/s), (b) represents the medium velocity (3.5 m/s) and (c) represents the high velocity (10 m/s).

Table 1. Separation efficiency based on mass for each case.

Case	Air velocity (m/s)	Liquid volume fraction (%)	φ (%)
I	1.0	1	99.991233
II		10	99.999925
III	3.5	1	99.997504
IV		10	99.999974
V	10	1	99.997475
VI		10	99.999926

Table 2. Separation efficiency based on number for each case.

Case	Air velocity (m/s)	Liquid volume fraction (%)	φ_{number} (%)
I	1.0	1	91.47
II		10	98.74
III	3.5	1	91.14
IV		10	99.11
V	10	1	91.45
VI		10	97.50

The results show some important differences between mass and number efficiencies. While the mass separation efficiency shows higher values close to each other, the number separation efficiency exhibits lower values with higher

variation between them. This is mainly explained by the fact that wave-plate demisters are very efficient equipment, especially at separating larger drops. The smaller droplets tend to escape more from the outlet but represent a small portion of the total mass that entered the domain. The case IV is considered the best condition for separating liquid droplets since it resulted in a number separation efficiency of 99.11%, showing that the equipment of this study works at best at medium velocities, around 3.5 m/s. Between the low and high velocities (1.0 and 10 m/s, respectively), the low velocity showed better separation efficiencies.

4. CONCLUSION

A numerical study of mist elimination process was conducted using LES approach and the demister performance was evaluated. For this purpose, numerical simulations were conducted considering Eulerian-Lagrangian method for the two-phase flow and WALE turbulence model for the LES sub-grid scales, while using three air velocities (1.0, 3.5 and 10 m/s) and two liquid volume fractions (1 and 10%). A mesh quality analysis was also performed. Some interesting conclusions can be listed below:

- Higher flow velocities produce higher turbulence energy spectra with larger eddies when compared to low velocities. These larger eddies tend to be more easily captured/resolved by the mesh, as enough spatial resolution is provided;
- The demister used in this study works at best with higher concentration of droplets around 10% of volume fraction and at medium velocities around 3.5 m/s, reaching a number separation efficiency of 99.11%. Between the low and high velocities (1.0 and 10 m/s, respectively), the low velocity showed better separation efficiencies;
- Mass separation efficiency is not indicated for evaluating the performance of wave-plate demisters, since smaller droplets represent only a small portion of the total mass and this equipment is less efficient in separating these smaller droplets.

5. ACKNOWLEDGEMENTS

The authors are grateful for the financial support of PETROBRAS for this research paper, through the cooperation agreement number 0050.0119786.21.9.

6. REFERENCES

Guan, L. et al., 2016. “Numerical Study on the Penetration of Droplets in a Zigzag Demister”. *Environmental Engineering Science*, v. 33, n. 1, p. 35-43. <http://dx.doi.org/10.1089/ees.2014.0367>.

James, P.W. et al., 2003. “The Role of Drainage Channels in the Performance of Wave-Plate Mist Eliminators”. *Chemical Engineering Research And Design*, v. 81, n. 6, p. 639-648. <http://dx.doi.org/10.1205/026387603322150499>.

Kavousi, F.; Behjat, Y. and Shahhosseini, S., 2013. “Optimal design of drainage channel geometry parameters in vane demister liquid–gas separators”. *Chemical Engineering Research And Design*, v. 91, n. 7, p. 1212-1222. <http://dx.doi.org/10.1016/j.cherd.2013.01.012>.

Li, S. et al., 2020. “Numerical analysis of chevron demisters with drainage hooks in optimizing separation performance”. *International Journal Of Heat And Mass Transfer*, Vol. 152, p. 119522. <http://dx.doi.org/10.1016/j.ijheatmasstransfer.2020.119522>.

Pope, S. B., 2000. *Turbulent Flows.* Cambridge University Press.

Stewart, M. and Arnold, K., 2008. *Gas-Liquid and Liquid-Liquid Separators*. Burlington: Elsevier.

Venkatesan, G., Kulasekharan, N. and Iniyan, S., 2014. “Numerical analysis of curved vane demisters in estimating water droplet separation efficiency”. *Desalination*, v. 339, p. 40-53. <http://dx.doi.org/10.1016/j.desal.2014.02.013>.

Wang, Y.I. and James, P.W., 1998. “The Calculation of Wave-Plate Demister Efficiencies Using Numerical Simulation of the Flow Field and Droplet Motion”. *Chemical Engineering Research And Design*, v. 76, n. 8, p. 980-985. <http://dx.doi.org/10.1205/026387698525630>.

Yang, L. et al., 2021. “Experimental and numerical analysis of a demister with vortex generators”. *Chinese Journal Of Chemical Engineering*, v. 33, p. 83-95. <http://dx.doi.org/10.1016/j.cjche.2020.07.045>.

Zhao, J; Jin, B and Zhong, Z., 2007. “Study of the separation efficiency of a demister vane with response surface methodology”. *Journal Of Hazardous Materials*, v. 147, n. 1-2, p. 363-369. <http://dx.doi.org/10.1016/j.jhazmat.2007.01.046>.

7. RESPONSIBILITY NOTICE

The authors are the only responsible for the printed material included in this paper.